

## Committer functions for climate problems and how to compute them

**Corentin Herbert**  
CNRS, ENS de Lyon, France

April 29, 2022 — Critical Earth Workshop, Berg en Dal, Netherlands

With: Dario Lucente, Freddy Bouchet, Joran Rolland.

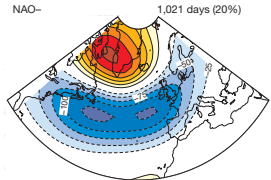


# Outline

- 1 Introduction: Committor functions for Prediction Problems and Climate Transitions
- 2 Climate prediction at the predictability margin
- 3 Data-based methods for committer function computation
- 4 Rare events and committer functions
- 5 Conclusion

# Examples of prediction problems on sub-seasonal to decadal time scales

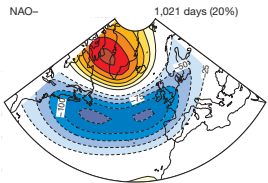
## North Atlantic Oscillation



C. Cassou (2008). *Nature*

# Examples of prediction problems on sub-seasonal to decadal time scales

## North Atlantic Oscillation



C. Cassou (2008). *Nature*

## El Niño

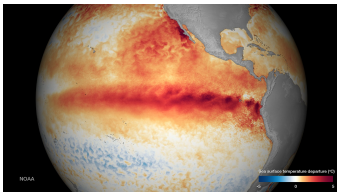
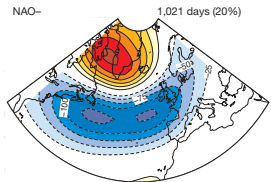


Image: NOAA

# Examples of prediction problems on sub-seasonal to decadal time scales

## North Atlantic Oscillation



C. Cassou (2008). *Nature*

## El Niño

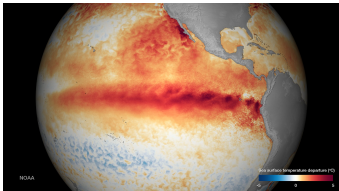


Image: NOAA

## 2003 European Heat Wave

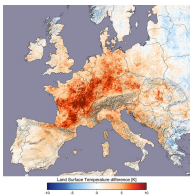
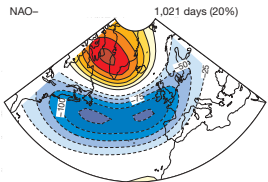


Image: NASA

# Examples of prediction problems on sub-seasonal to decadal time scales

## North Atlantic Oscillation



C. Cassou (2008). *Nature*

## El Niño

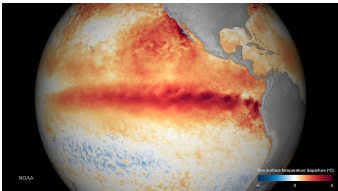


Image: NOAA

## 2003 European Heat Wave

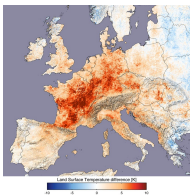


Image: NASA

## Renewable energy shortfalls

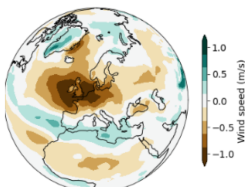
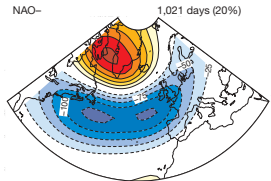


Image: B. Cozian

Examples of prediction problems on sub-seasonal to decadal time scales

## North Atlantic Oscillation



C. Cassou (2008). *Nature*

## El Niño

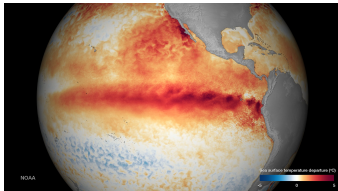


Image: NOAA

## 2003 European Heat Wave

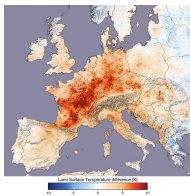


Image: NASA

## **Renewable energy shortfalls**

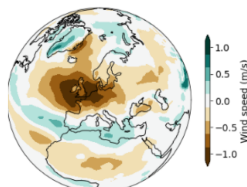


Image: B. Cozian

*Can we estimate the probability of occurrence of such events, given the current state of the system?*

# The structure of Climate Prediction Problems

## Weather Forecasting



*Strongly dependent on  
the initial condition!*

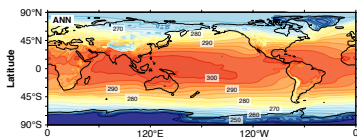
# The structure of Climate Prediction Problems

## Weather Forecasting



*Strongly dependent on  
the initial condition!*

## Climatology



*Property of the invariant  
measure.*

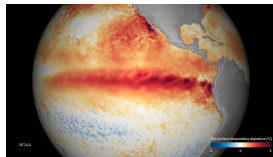
# The structure of Climate Prediction Problems

## Weather Forecasting



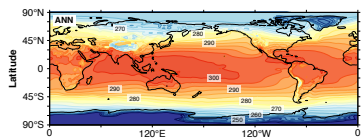
*Strongly dependent on the initial condition!*

## Climate Prediction



*Probabilistic prediction, still depends on initial condition*

## Climatology



*Property of the invariant measure.*

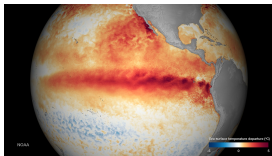
# The structure of Climate Prediction Problems

## Weather Forecasting



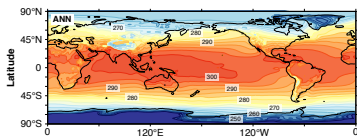
*Strongly dependent on the initial condition!*

## Climate Prediction

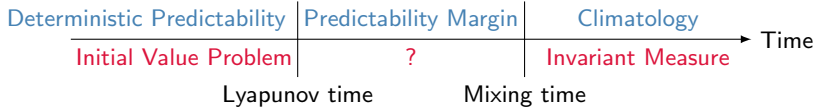


*Probabilistic prediction, still depends on initial condition*

## Climatology



*Property of the invariant measure.*



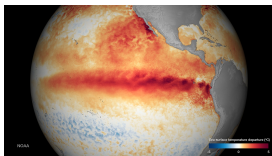
# The structure of Climate Prediction Problems

## Weather Forecasting



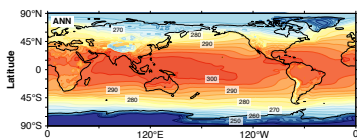
*Strongly dependent on the initial condition!*

## Climate Prediction

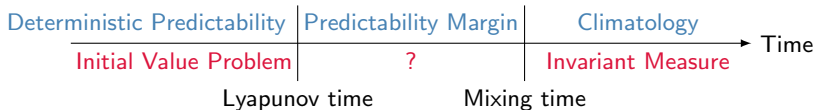


*Probabilistic prediction, still depends on initial condition*

## Climatology



*Property of the invariant measure.*



Typically we want to estimate quantities such as:

$$\mathbb{P} \left[ \sup_{0 \leq t \leq T} A[X_t] > a | X_0 = x \right], \text{ or } \mathbb{P} [A[X_T] > a | X_0 = x].$$

Examples of observables: NAO or ENSO index, Temperature anomaly over Europe (heat waves),...

# The case of rare events

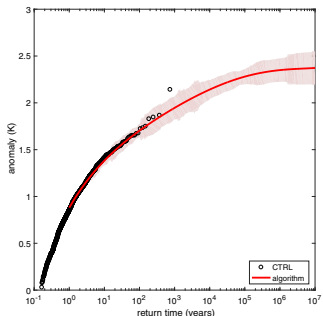
For rare events, climatological properties are themselves difficult to estimate (e.g. *return times*). The ability to make predictions conditioned on initial state can help, using *rare event algorithms*<sup>1</sup>.

<sup>1</sup>T. Lestang, F. Ragone, C.-E. Bréhier, C. Herbert, and F. Bouchet (2018). *J. Stat. Mech.*

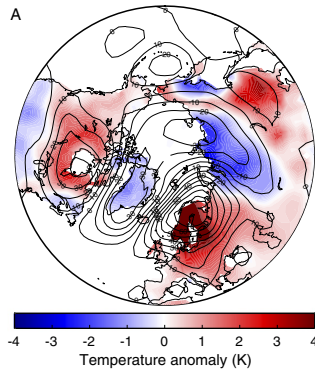
## The case of rare events

For rare events, climatological properties are themselves difficult to estimate (e.g. *return times*). The ability to make predictions conditioned on initial state can help, using *rare event algorithms*<sup>1</sup>.

## Return time plot for 90-day temperature anomaly over Europe.



## Composite temperature and geopotential map for 90-days heat waves with amplitude 2K.



F. Ragone, J. Wouters, and F. Bouchet (2018). *Proc. Natl. Acad. Sci. U.S.A.*

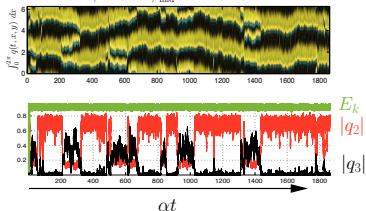
<sup>1</sup>T. Lestang, F. Ragone, C.-E. Bréhier, C. Herbert, and F. Bouchet (2018). *J. Stat. Mech.*

# Transitions between Climate Attractors

# Transitions between Climate Attractors

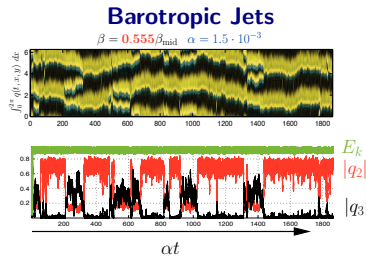
## Barotropic Jets

$$\beta = 0.555\beta_{\text{mid}} \quad \alpha = 1.5 \cdot 10^{-3}$$

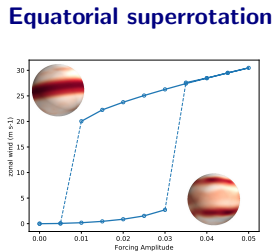


F. Bouchet, J. Rolland, and E. Simonnet (2019). *Phys. Rev. Lett.*

# Transitions between Climate Attractors

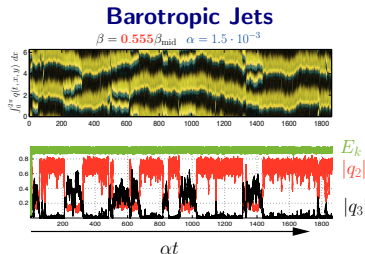


F. Bouchet, J. Rolland, and E. Simonnet (2019). *Phys. Rev. Lett.*



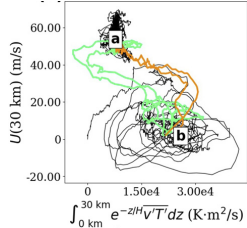
C. Herbert, R. Caballero, and F. Bouchet (2020). *J. Atmos. Sci.*

# Transitions between Climate Attractors

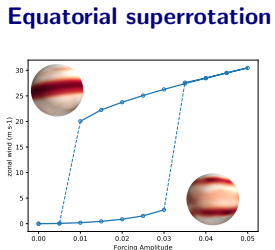


F. Bouchet, J. Rolland, and E. Simonnet (2019). *Phys. Rev. Lett.*

## Sudden Stratospheric Warmings

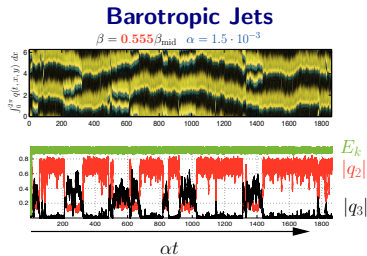


J. Finkel et al. (2021). Mon. Wea. Rev.



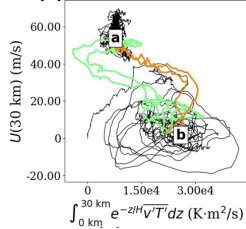
C. Herbert, R. Caballero, and F. Bouchet (2020). *J. Atmos. Sci.*

# Transitions between Climate Attractors

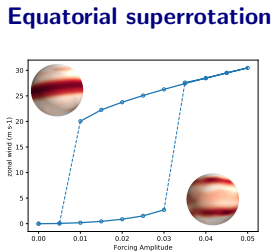


F. Bouchet, J. Rolland, and E. Simonnet (2019). *Phys. Rev. Lett.*

## Sudden Stratospheric Warnings

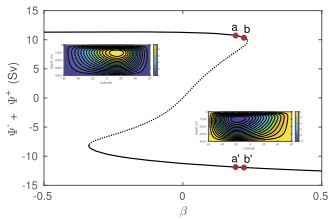


J. Finkel et al. (2021). Mon. Wea. Rev.



C. Herbert, R. Caballero, and F. Bouchet (2020). *J. Atmos. Sci.*

## AMOC collapse



S. Baars, D Castellana, F. W. Wubs, and H. A. Dijkstra (2021). *J. Comput. Phys.*

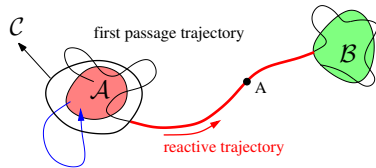
# Committor function

Markov process  $(X_t)_{t \geq 0}$

Committor function<sup>2</sup>:

$$q(x) = \text{Prob}[\tau_B < \tau_A | X_0 = x],$$

with  $\tau_C = \inf\{t > 0 | X_t \in \mathcal{C}\}$ .



<sup>2</sup>E. Vanden-Eijnden (2006). In: *Computer Simulations in Condensed Matter Systems: From Materials to Chemical Biology Volume 1*. Springer; P. Metzner, C. Schütte, and E. Vanden-Eijnden (2006). *J. Chem. Phys.*

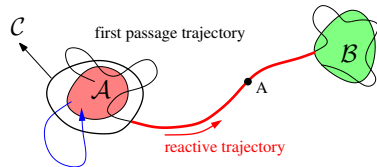
# Committor function

Markov process  $(X_t)_{t \geq 0}$

*Committor function*<sup>2</sup>:

$$q(x) = \text{Prob}[\tau_B < \tau_A | X_0 = x],$$

with  $\tau_C = \inf\{t > 0 | X_t \in \mathcal{C}\}$ .



## Prediction problems as committor functions:

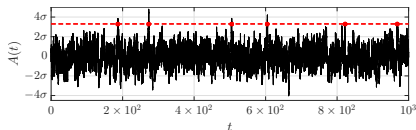
$$Y_t = (t, O[X, t]),$$

$$\mathcal{A} = \{(T, z), z \leq a\},$$

$$\mathcal{B} = \{(t, z), 0 \leq t \leq T, z > a\},$$

for some observable  $O$ , threshold  $a$  and observation time  $T$ . Then

$$q(x) = \text{Prob} \left[ \max_{0 \leq t \leq T} O[X, t] > a \right].$$



T. Lestang, F. Ragone, C.-E. Bréhier, C. Herbert, and F. Bouchet

(2018). *J. Stat. Mech.*

<sup>2</sup>E. Vanden-Eijnden (2006). In: *Computer Simulations in Condensed Matter Systems: From Materials to Chemical Biology Volume 1*. Springer; P. Metzner, C. Schütte, and E. Vanden-Eijnden (2006). *J. Chem. Phys.*

## Main questions

- ▶ Is the probability of occurrence of events at the predictability margin really predictable?
- Does the spatial structure of the committor function affect predictability?

# Main questions

- ▶ Is the probability of occurrence of events at the predictability margin really predictable?  
Does the spatial structure of the committor function affect predictability?
- ▶ How to estimate committor functions?  
From models? From data?

## Main questions

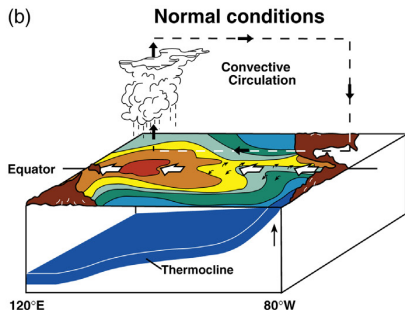
- ▶ Is the probability of occurrence of events at the predictability margin really predictable?  
Does the spatial structure of the committor function affect predictability?
- ▶ How to estimate committor functions?  
From models? From data?
- ▶ Can we use data-based committor function estimates to improve rare event algorithms?

# Outline

- 1 Introduction: Committor functions for Prediction Problems and Climate Transitions
- 2 Climate prediction at the predictability margin
- 3 Data-based methods for committor function computation
- 4 Rare events and committor functions
- 5 Conclusion

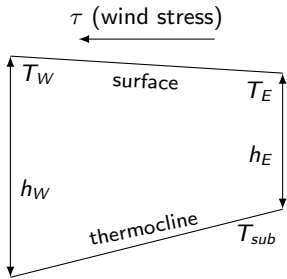
# The Jin-Timmermann model<sup>3</sup> of ENSO

(b)



<sup>3</sup>F.-F. Jin (1997a). *J. Atmos. Sci.*; F.-F. Jin (1997b). *J. Atmos. Sci.*; A. Timmermann and F.-F. Jin (2002). *Geophys. Res. Lett.*; A. Timmermann, F.-F. Jin, and J. Abshagen (2003). *J. Atmos. Sci.*

# The Jin-Timmermann model<sup>3</sup> of ENSO



3-degrees of freedom model:

$$\frac{dT_W}{dt} = -\alpha(T_W - T_r) - \epsilon\beta\tau(1 - \sigma\eta_t)(T_E - T_W),$$

$$\frac{dT_E}{dt} = -\alpha(T_E - T_r) + \zeta\beta\tau(1 - \sigma\eta_t)(T_E - T_{sub}),$$

$$\frac{dh_W}{dt} = r \left( -h_W - \frac{1}{2}bL\tau \right),$$

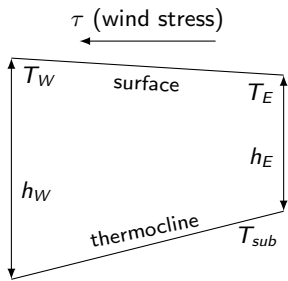
$$T_{sub} = \frac{T_r + T_{r0}}{2} + \frac{T_r - T_{r0}}{2} \tanh \left( \frac{H + h_E - z_0}{h^*} \right),$$

$$\tau = \frac{\mu(T_E - T_W)}{\beta},$$

$$h_E = h_W + bL\tau.$$

<sup>3</sup>F.-F. Jin (1997a). *J. Atmos. Sci.*; F.-F. Jin (1997b). *J. Atmos. Sci.*; A. Timmermann and F.-F. Jin (2002). *Geophys. Res. Lett.*; A. Timmermann, F.-F. Jin, and J. Abschagen (2003). *J. Atmos. Sci.*

# The Jin-Timmermann model<sup>3</sup> of ENSO



► Newtonian relaxation

3-degrees of freedom model:

$$\frac{dT_W}{dt} = -\alpha(T_W - T_r) - \epsilon\beta\tau(1 - \sigma\eta_t)(T_E - T_W),$$

$$\frac{dT_E}{dt} = -\alpha(T_E - T_r) + \zeta\beta\tau(1 - \sigma\eta_t)(T_E - T_{sub}),$$

$$\frac{dh_W}{dt} = r \left( -h_W - \frac{1}{2}bL\tau \right),$$

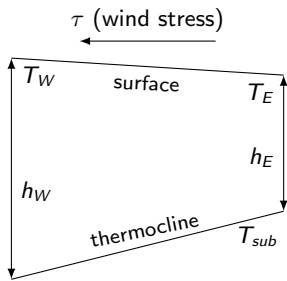
$$T_{sub} = \frac{T_r + T_{r0}}{2} + \frac{T_r - T_{r0}}{2} \tanh \left( \frac{H + h_E - z_0}{h^*} \right),$$

$$\tau = \frac{\mu(T_E - T_W)}{\beta},$$

$$h_E = h_W + bL\tau.$$

<sup>3</sup>F.-F. Jin (1997a). *J. Atmos. Sci.*; F.-F. Jin (1997b). *J. Atmos. Sci.*; A. Timmermann and F.-F. Jin (2002). *Geophys. Res. Lett.*; A. Timmermann, F.-F. Jin, and J. Abschagen (2003). *J. Atmos. Sci.*

# The Jin-Timmermann model<sup>3</sup> of ENSO



- ▶ Newtonian relaxation
- ▶ Zonal advection

3-degrees of freedom model:

$$\frac{dT_W}{dt} = -\alpha(T_W - T_r) - \epsilon\beta\tau(1 - \sigma\eta_t)(T_E - T_W),$$

$$\frac{dT_E}{dt} = -\alpha(T_E - T_r) + \zeta\beta\tau(1 - \sigma\eta_t)(T_E - T_{sub}),$$

$$\frac{dh_W}{dt} = r \left( -h_W - \frac{1}{2}bL\tau \right),$$

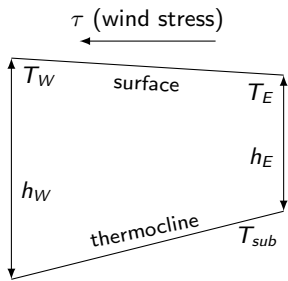
$$T_{sub} = \frac{T_r + T_{r0}}{2} + \frac{T_r - T_{r0}}{2} \tanh \left( \frac{H + h_E - z_0}{h^*} \right),$$

$$\tau = \frac{\mu(T_E - T_W)}{\beta},$$

$$h_E = h_W + bL\tau.$$

<sup>3</sup>F.-F. Jin (1997a). *J. Atmos. Sci.*; F.-F. Jin (1997b). *J. Atmos. Sci.*; A. Timmermann and F.-F. Jin (2002). *Geophys. Res. Lett.*; A. Timmermann, F.-F. Jin, and J. Abschagen (2003). *J. Atmos. Sci.*

# The Jin-Timmermann model<sup>3</sup> of ENSO



- ▶ Newtonian relaxation
- ▶ Zonal advection
- ▶ Upwelling

3-degrees of freedom model:

$$\frac{dT_W}{dt} = -\alpha(T_W - T_r) - \epsilon\beta\tau(1 - \sigma\eta_t)(T_E - T_W),$$

$$\frac{dT_E}{dt} = -\alpha(T_E - T_r) + \zeta\beta\tau(1 - \sigma\eta_t)(T_E - T_{sub}),$$

$$\frac{dh_W}{dt} = r \left( -h_W - \frac{1}{2}bL\tau \right),$$

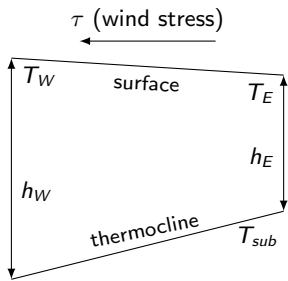
$$T_{sub} = \frac{T_r + T_{r0}}{2} + \frac{T_r - T_{r0}}{2} \tanh \left( \frac{H + h_E - z_0}{h^*} \right),$$

$$\tau = \frac{\mu(T_E - T_W)}{\beta},$$

$$h_E = h_W + bL\tau.$$

<sup>3</sup>F.-F. Jin (1997a). *J. Atmos. Sci.*; F.-F. Jin (1997b). *J. Atmos. Sci.*; A. Timmermann and F.-F. Jin (2002). *Geophys. Res. Lett.*; A. Timmermann, F.-F. Jin, and J. Abschagen (2003). *J. Atmos. Sci.*

# The Jin-Timmermann model<sup>3</sup> of ENSO



- ▶ Newtonian relaxation
- ▶ Zonal advection
- ▶ Upwelling
- ▶ Effect of wind stress on thermocline depth

3-degrees of freedom model:

$$\frac{dT_W}{dt} = -\alpha(T_W - T_r) - \epsilon\beta\tau(1 - \sigma\eta_t)(T_E - T_W),$$

$$\frac{dT_E}{dt} = -\alpha(T_E - T_r) + \zeta\beta\tau(1 - \sigma\eta_t)(T_E - T_{sub}),$$

$$\frac{dh_W}{dt} = r \left( -h_W - \frac{1}{2} bL\tau \right),$$

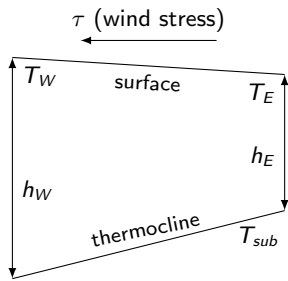
$$T_{sub} = \frac{T_r + T_{r0}}{2} + \frac{T_r - T_{r0}}{2} \tanh \left( \frac{H + h_E - z_0}{h^*} \right),$$

$$\tau = \frac{\mu(T_E - T_W)}{\beta},$$

$$h_E = h_W + bL\tau.$$

<sup>3</sup>F.-F. Jin (1997a). *J. Atmos. Sci.*; F.-F. Jin (1997b). *J. Atmos. Sci.*; A. Timmermann and F.-F. Jin (2002). *Geophys. Res. Lett.*; A. Timmermann, F.-F. Jin, and J. Abshagen (2003). *J. Atmos. Sci.*

# The Jin-Timmermann model<sup>3</sup> of ENSO



- ▶ Newtonian relaxation
- ▶ Zonal advection
- ▶ Upwelling
- ▶ Effect of wind stress on thermocline depth

3-degrees of freedom model:

$$\frac{dT_W}{dt} = -\alpha(T_W - T_r) - \epsilon\beta\tau(1 - \sigma\eta_t)(T_E - T_W),$$

$$\frac{dT_E}{dt} = -\alpha(T_E - T_r) + \zeta\beta\tau(1 - \sigma\eta_t)(T_E - T_{sub}),$$

$$\frac{dh_W}{dt} = r \left( -h_W - \frac{1}{2}bL\tau \right),$$

$$T_{sub} = \frac{T_r + T_{r0}}{2} + \frac{T_r - T_{r0}}{2} \tanh \left( \frac{H + h_E - z_0}{h^*} \right),$$

$$\tau = \frac{\mu(T_E - T_W)}{\beta},$$

$$h_E = h_W + bL\tau.$$

The model can be either deterministic ( $\sigma = 0$ ) or stochastic ( $\sigma > 0$ ).

<sup>3</sup>F.-F. Jin (1997a). *J. Atmos. Sci.*; F.-F. Jin (1997b). *J. Atmos. Sci.*; A. Timmermann and F.-F. Jin (2002). *Geophys. Res. Lett.*; A. Timmermann, F.-F. Jin, and J. Abschagen (2003). *J. Atmos. Sci.*

# Non-dimensional form of the Jin-Timmermann model<sup>4</sup>

From the problem parameters, one can construct a temperature and time scale  $T_0 = \frac{h^* \beta}{bL\mu}$  and  $t^* = \frac{bL}{\beta\zeta h^*}$ , and introduce non-dimensional variables:

$$\begin{aligned}x &= \frac{T_E - T_W}{T_0}, & y &= \frac{T_W - T_r}{T_0}, \\z &= \frac{h_W + H - z_0}{h^*}, & \tilde{t} &= \frac{t}{t^*},\end{aligned}$$

The non-dimensional equations become:

$$\begin{aligned}\dot{x} &= \rho\delta(x^2 - ax) + x[x + y + c - c\tanh(x + z)] - D_x(x, y, z)\eta_t, \\ \dot{y} &= -\rho\delta(x^2 + ay) + D_y(x, y, z)\eta_t, \\ \dot{z} &= \delta\left(k - z - \frac{x}{2}\right),\end{aligned}$$

where

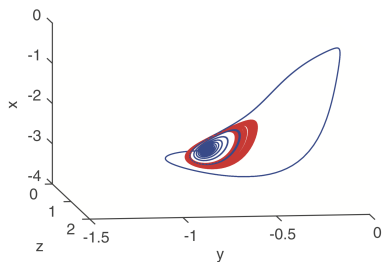
$$\begin{aligned}D_x(x, y, z) &= [(1 + \rho\delta)x^2 + xy + cx(1 - \tanh(x + z))] \sigma, \\ D_y(x, y, z) &= \rho\delta x^2 \sigma,\end{aligned}$$

and  $\delta, \rho, c, k, a$  are non-dimensional parameters.

<sup>4</sup>A. Roberts, J. Guckenheimer, E. Widiasih, A. Timmermann, and C. K. Jones (2016). *J. Atmos. Sci.*

# Coexistence of attractors in the Jin-Timmermann model

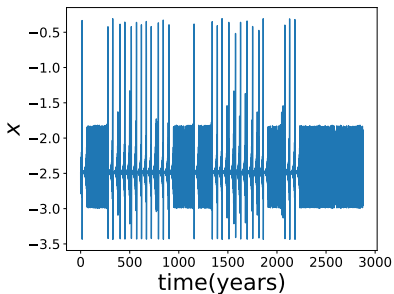
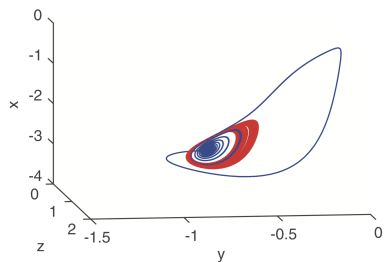
For a given choice of parameters, a periodic orbit and a chaotic attractor coexist in the deterministic model ( $\sigma = 0$ )<sup>5</sup>.



<sup>5</sup> J. Guckenheimer, A. Timmermann, H. Dijkstra, and A. Roberts (2017). *Dyn. Stat. Clim. Sys.*

# Coexistence of attractors in the Jin-Timmermann model

For a given choice of parameters, a periodic orbit and a chaotic attractor coexist in the deterministic model ( $\sigma = 0$ )<sup>5</sup>.



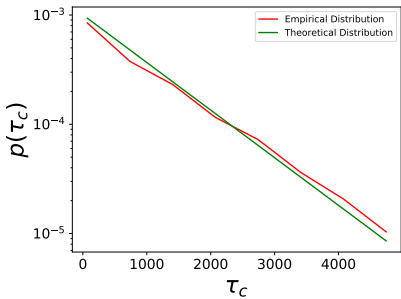
In the stochastic model ( $\sigma \neq 0$ ), spontaneous transitions to strong El Niño events occur in a seemingly random manner.

<sup>5</sup> J. Guckenheimer, A. Timmermann, H. Dijkstra, and A. Roberts (2017). *Dyn. Stat. Clim. Sys.*

# Statistics of transitions to strong El Niño regimes

## First-passage time

$$\tau_c(\mathbf{x}) = \inf\{t > 0 : x(t) > -1 \mid \mathbf{X}(0) = \mathbf{x}\}.$$

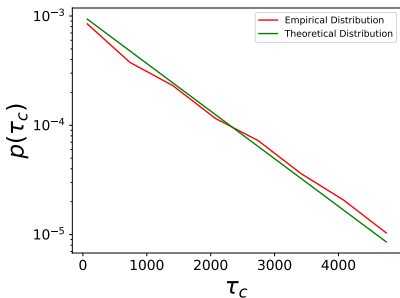


First-passage time has an exponential distribution  $p(\tau_c) = \lambda e^{-\lambda \tau_c}$ .

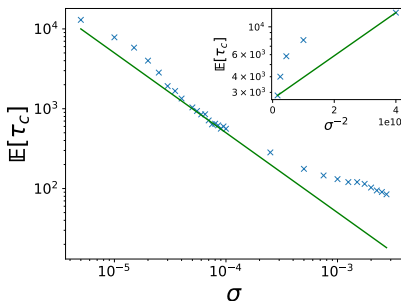
# Statistics of transitions to strong El Niño regimes

## First-passage time

$$\tau_c(\mathbf{x}) = \inf\{t > 0 : x(t) > -1 \mid \mathbf{X}(0) = \mathbf{x}\}.$$



First-passage time has an exponential distribution  $p(\tau_c) = \lambda e^{-\lambda \tau_c}$ .



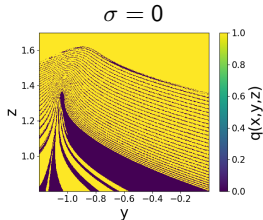
But it does not obey an Arrhenius law ( $(E[\tau_c])_{\sigma \rightarrow 0} \sim Ae^{\frac{\Delta V}{\sigma^2}}$ ).

# Committor function for the Jin-Timmermann model<sup>6</sup>

*What is the probability that a strong El Niño event occurs within a given timeframe, given the state of the system at the time of prediction?*

$$q(\mathbf{x}) = \mathbb{P} \left( \max_{0 \leq t \leq T} x(t) > -1 \mid \mathbf{X}(0) = \mathbf{x} \right).$$

**Direct estimate of the committor function in the plane  $x = -2.831$ :**  
( $T=200$ , 1000 trajectories per cell)



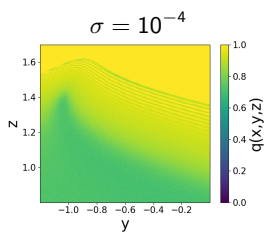
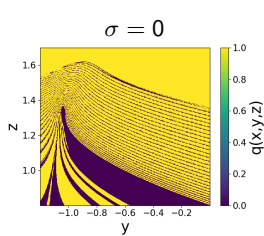
<sup>6</sup>D. Luente, C. Herbert, and F. Bouchet (submitted). *J. Atmos. Sci.*

# Committor function for the Jin-Timmermann model<sup>6</sup>

*What is the probability that a strong El Niño event occurs within a given timeframe, given the state of the system at the time of prediction?*

$$q(\mathbf{x}) = \mathbb{P} \left( \max_{0 \leq t \leq T} x(t) > -1 \mid \mathbf{X}(0) = \mathbf{x} \right).$$

**Direct estimate of the committor function in the plane  $x = -2.831$ :**  
(T=200, 1000 trajectories per cell)



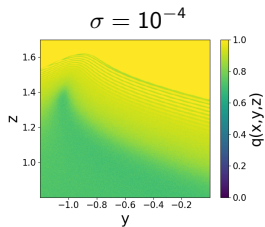
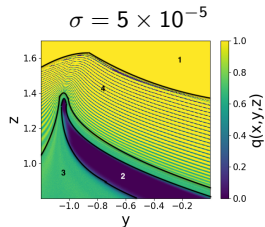
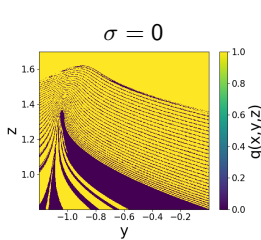
<sup>6</sup>D. Luente, C. Herbert, and F. Bouchet (submitted). *J. Atmos. Sci.*

# Committor function for the Jin-Timmermann model<sup>6</sup>

*What is the probability that a strong El Niño event occurs within a given timeframe, given the state of the system at the time of prediction?*

$$q(\mathbf{x}) = \mathbb{P} \left( \max_{0 \leq t \leq T} x(t) > -1 \mid \mathbf{X}(0) = \mathbf{x} \right).$$

**Direct estimate of the committor function in the plane  $x = -2.831$ :**  
( $T=200$ , 1000 trajectories per cell)



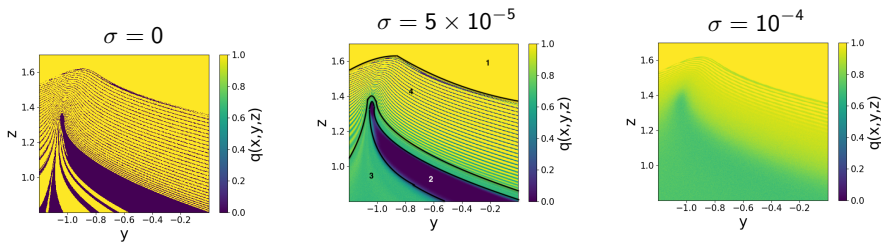
<sup>6</sup>D. Luente, C. Herbert, and F. Bouchet (submitted). *J. Atmos. Sci.*

# Committor function for the Jin-Timmermann model<sup>6</sup>

*What is the probability that a strong El Niño event occurs within a given timeframe, given the state of the system at the time of prediction?*

$$q(\mathbf{x}) = \mathbb{P} \left( \max_{0 \leq t \leq T} x(t) > -1 \mid \mathbf{X}(0) = \mathbf{x} \right).$$

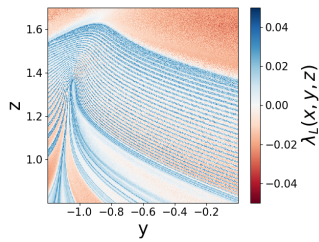
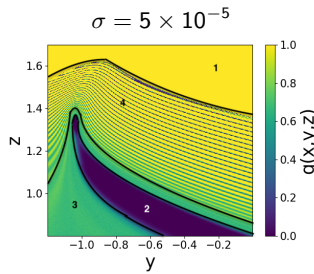
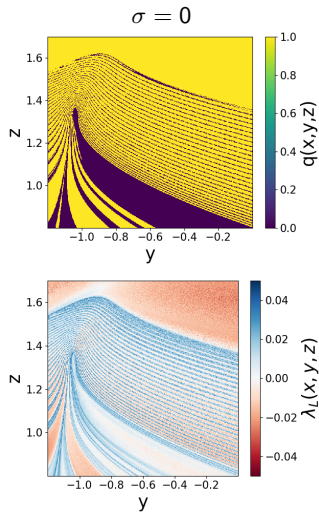
**Direct estimate of the committor function in the plane  $x = -2.831$ :**  
(T=200, 1000 trajectories per cell)



*There exists a region in phase space where the probability of occurrence is predictable.*

<sup>6</sup>D. Luente, C. Herbert, and F. Bouchet (submitted). *J. Atmos. Sci.*

# Characterization of probabilistically predictable regions<sup>7</sup>

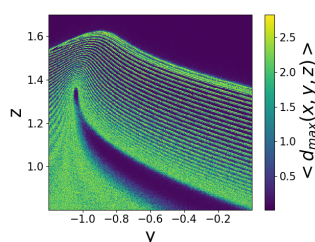
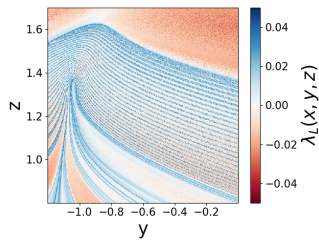
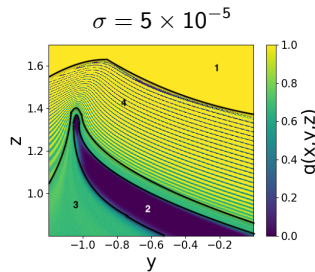
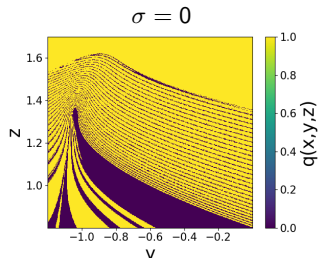


Finite time Lyapunov exponent

$$\lambda_L = \frac{1}{T} \log \left( \frac{\Delta(T)}{\Delta(0)} \right)$$

<sup>7</sup>D. Luente, C. Herbert, and F. Bouchet (submitted). *J. Atmos. Sci.*

# Characterization of probabilistically predictable regions<sup>7</sup>



Finite time Lyapunov exponent  
 $\lambda_L = \frac{1}{T} \log \left( \frac{\Delta(T)}{\Delta(0)} \right)$

$$\langle d_{\max} \rangle = \langle \max_{t \in [0, T]} \| \mathbf{x}_1(t) - \mathbf{x}_2(t) \|^2 \rangle$$

<sup>7</sup> D. Luente, C. Herbert, and F. Bouchet (submitted). *J. Atmos. Sci.*

# Outline

- 1 Introduction: Committor functions for Prediction Problems and Climate Transitions
- 2 Climate prediction at the predictability margin
- 3 Data-based methods for committer function computation
- 4 Rare events and committer functions
- 5 Conclusion

# Computing committor functions from a model

- ▶ Direct sampling on discretized phase space (see previous section)

$$\hat{q} = \frac{N_{\mathcal{B}}}{N}.$$

Computational cost grows exponentially with dimension.

# Computing committor functions from a model

- ▶ Direct sampling on discretized phase space (see previous section)

$$\hat{q} = \frac{N_{\mathcal{B}}}{N}.$$

Computational cost grows exponentially with dimension.

- ▶ Solving the backward Kolmogorov equation

For a diffusion process  $dX_t = b(X_t)dt + \sigma(X_t)dW_t$ , the committor is a solution of the PDE:

$$0 = b(x) \cdot \nabla q(x) + \frac{1}{2}(\sigma(x)\sigma(x)^T) : \nabla\nabla q(x),$$

with boundary conditions

$$q|_{\partial\mathcal{A}} = 0, \quad q|_{\partial\mathcal{B}} = 1.$$

# Computing committor functions from a model

- ▶ Direct sampling on discretized phase space (see previous section)

$$\hat{q} = \frac{N_{\mathcal{B}}}{N}.$$

Computational cost grows exponentially with dimension.

- ▶ Solving the backward Kolmogorov equation

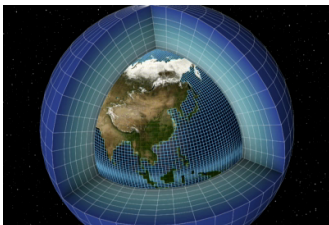
For a diffusion process  $dX_t = b(X_t)dt + \sigma(X_t)dW_t$ , the committor is a solution of the PDE:

$$0 = b(x) \cdot \nabla q(x) + \frac{1}{2}(\sigma(x)\sigma(x)^T) : \nabla\nabla q(x),$$

with boundary conditions

$$q|_{\partial\mathcal{A}} = 0, \quad q|_{\partial\mathcal{B}} = 1.$$

*These methods do not generalize to large dimension!*



# Computing the committor function from a trajectory<sup>8</sup>

Sample trajectory  $\{\mathbf{X}_n\}_{1 \leq n \leq N}$ .

## Direct estimator of the committor function

$$\hat{\rho}_N(\mathbf{x}) \hat{q}_N(\mathbf{x}) = \frac{1}{N} \sum_{n=1}^N \delta(\mathbf{X}_n - \mathbf{x}) \mathbf{1}_{\{\tau_B(\mathbf{x}_n) \leq \tau_A(\mathbf{x}_n)\}},$$

$$\hat{\rho}_N(\mathbf{x}) = \frac{1}{N} \sum_{n=1}^N \delta(\mathbf{X}_n - \mathbf{x}).$$

<sup>8</sup>L. J. Lopes and T. Lelièvre (2019). *Journal of computational chemistry*; D. Lucente, S. Duffner, C. Herbert, J. Rolland, and F. Bouchet (2019). In: *Proceedings of the 9th International Workshop on Climate Informatics: CI 2019* (Paris). Ed. by J. Brajard, A. Charantonis, C. Chen, and J. Runge. NCAR; D. Lucente, C. Herbert, and F. Bouchet (submitted). *J. Atmos. Sci.*

# Computing the committor function from a trajectory<sup>8</sup>

Sample trajectory  $\{\mathbf{X}_n\}_{1 \leq n \leq N}$ .

## Direct estimator of the committor function

$$\hat{\rho}_N(\mathbf{x}) \hat{q}_N(\mathbf{x}) = \frac{1}{N} \sum_{n=1}^N \delta(\mathbf{X}_n - \mathbf{x}) \mathbf{1}_{\{\tau_B(\mathbf{x}_n) \leq \tau_A(\mathbf{x}_n)\}},$$
$$\hat{\rho}_N(\mathbf{x}) = \frac{1}{N} \sum_{n=1}^N \delta(\mathbf{X}_n - \mathbf{x}).$$

## Extend the committor function to the whole space

- For point  $\mathbf{y} \in \mathbb{R}^D$ , find  $K$  nearest neighbors  $\mathbf{X}_{n_1}, \dots, \mathbf{X}_{n_K}$  in sample trajectory.

<sup>8</sup>L. J. Lopes and T. Lelièvre (2019). *Journal of computational chemistry*; D. Lucente, S. Duffner, C. Herbert, J. Rolland, and F. Bouchet (2019). In: *Proceedings of the 9th International Workshop on Climate Informatics: CI 2019* (Paris). Ed. by J. Brajard, A. Charantonis, C. Chen, and J. Runge. NCAR; D. Lucente, C. Herbert, and F. Bouchet (submitted). *J. Atmos. Sci.*

# Computing the committor function from a trajectory<sup>8</sup>

Sample trajectory  $\{\mathbf{X}_n\}_{1 \leq n \leq N}$ .

## Direct estimator of the committor function

$$\hat{\rho}_N(\mathbf{x}) \hat{q}_N(\mathbf{x}) = \frac{1}{N} \sum_{n=1}^N \delta(\mathbf{X}_n - \mathbf{x}) \mathbf{1}_{\{\tau_B(\mathbf{x}_n) \leq \tau_A(\mathbf{x}_n)\}},$$

$$\hat{\rho}_N(\mathbf{x}) = \frac{1}{N} \sum_{n=1}^N \delta(\mathbf{X}_n - \mathbf{x}).$$

## Extend the committor function to the whole space

- ▶ For point  $\mathbf{y} \in \mathbb{R}^D$ , find  $K$  nearest neighbors  $\mathbf{X}_{n_1}, \dots, \mathbf{X}_{n_K}$  in sample trajectory.
- ▶ Compute

$$\hat{q}_N(\mathbf{y}) = \frac{\sum_{k=1}^K w_k \hat{q}_N(\mathbf{X}_{n_k})}{\sum_{k=1}^K w_k}.$$

E.g.  $w_k = 1$  (uniform weights) or  $w_k = e^{-\|\mathbf{y} - \mathbf{X}_{n_k}\|^2/\omega^2}$  (Gaussian kernel).

<sup>8</sup>L. J. Lopes and T. Lelièvre (2019). *Journal of computational chemistry*; D. Lucente, S. Duffner, C. Herbert, J. Rolland, and F. Bouchet (2019). In: *Proceedings of the 9th International Workshop on Climate Informatics: CI 2019* (Paris). Ed. by J. Brajard, A. Charantonis, C. Chen, and J. Runge. NCAR; D. Lucente, C. Herbert, and F. Bouchet (submitted). *J. Atmos. Sci.*

# Computing the committor function from a trajectory<sup>8</sup>

Sample trajectory  $\{\mathbf{X}_n\}_{1 \leq n \leq N}$ .

## Direct estimator of the committor function

$$\hat{\rho}_N(\mathbf{x}) \hat{q}_N(\mathbf{x}) = \frac{1}{N} \sum_{n=1}^N \delta(\mathbf{X}_n - \mathbf{x}) \mathbf{1}_{\{\tau_B(\mathbf{x}_n) \leq \tau_A(\mathbf{x}_n)\}},$$

$$\hat{\rho}_N(\mathbf{x}) = \frac{1}{N} \sum_{n=1}^N \delta(\mathbf{X}_n - \mathbf{x}).$$

## Extend the committor function to the whole space

- ▶ For point  $\mathbf{y} \in \mathbb{R}^D$ , find  $K$  nearest neighbors  $\mathbf{X}_{n_1}, \dots, \mathbf{X}_{n_K}$  in sample trajectory.
- ▶ Compute

$$\hat{q}_N(\mathbf{y}) = \frac{\sum_{k=1}^K w_k \hat{q}_N(\mathbf{X}_{n_k})}{\sum_{k=1}^K w_k}.$$

E.g.  $w_k = 1$  (uniform weights) or  $w_k = e^{-\|\mathbf{y} - \mathbf{X}_{n_k}\|^2/\omega^2}$  (Gaussian kernel).

<sup>8</sup>L. J. Lopes and T. Lelièvre (2019). *Journal of computational chemistry*; D. Lucente, S. Duffner, C. Herbert, J. Rolland, and F. Bouchet (2019). In: *Proceedings of the 9th International Workshop on Climate Informatics: CI 2019* (Paris). Ed. by J. Brajard, A. Charantonis, C. Chen, and J. Runge. NCAR; D. Lucente, C. Herbert, and F. Bouchet (submitted). *J. Atmos. Sci.*

# Computing the committor function from a trajectory<sup>8</sup>

Sample trajectory  $\{\mathbf{X}_n\}_{1 \leq n \leq N}$ .

## Direct estimator of the committor function

$$\hat{\rho}_N(\mathbf{x}) \hat{q}_N(\mathbf{x}) = \frac{1}{N} \sum_{n=1}^N \delta(\mathbf{X}_n - \mathbf{x}) \mathbf{1}_{\{\tau_B(\mathbf{x}_n) \leq \tau_A(\mathbf{x}_n)\}},$$

$$\hat{\rho}_N(\mathbf{x}) = \frac{1}{N} \sum_{n=1}^N \delta(\mathbf{X}_n - \mathbf{x}).$$

## Extend the committor function to the whole space

- ▶ For point  $\mathbf{y} \in \mathbb{R}^D$ , find  $K$  nearest neighbors  $\mathbf{X}_{n_1}, \dots, \mathbf{X}_{n_K}$  in sample trajectory.
- ▶ Compute

$$\hat{q}_N(\mathbf{y}) = \frac{\sum_{k=1}^K w_k \hat{q}_N(\mathbf{X}_{n_k})}{\sum_{k=1}^K w_k}.$$

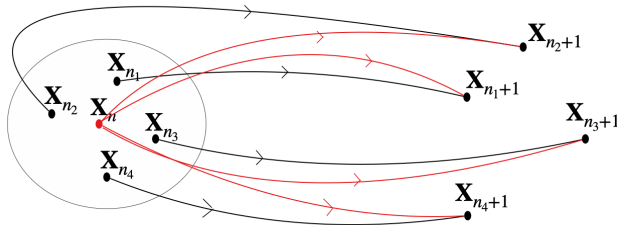
E.g.  $w_k = 1$  (uniform weights) or  $w_k = e^{-\|\mathbf{y} - \mathbf{X}_{n_k}\|^2/\omega^2}$  (Gaussian kernel).

This only uses the effectively observed transitions. Is it possible to extract more information about the dynamics from the observed trajectory?

<sup>8</sup>L. J. Lopes and T. Lelièvre (2019). *Journal of computational chemistry*; D. Luente, S. Duffner, C. Herbert, J. Rolland, and F. Bouchet (2019). In: *Proceedings of the 9th International Workshop on Climate Informatics: CI 2019* (Paris). Ed. by J. Brajard, A. Charantonis, C. Chen, and J. Runge. NCAR; D. Luente, C. Herbert, and F. Bouchet (submitted). *J. Atmos. Sci.*

# The Analogue Markov Chain<sup>9</sup>

Sample trajectory  $\{X_n\}_{1 \leq n \leq N}$ .



We define a Markov process whose states are the observed data points and with transition matrix defined as follows:

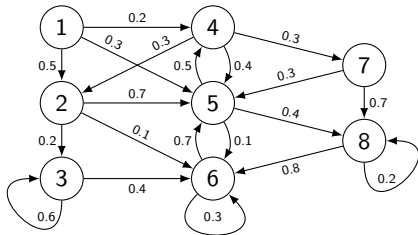
- ▶ For each  $1 \leq n \leq N$ , find the  $K$ -nearest neighbors  $\hat{X}_n^{(k)} = X_{n_k}$
- ▶ Assign transition probability  $p(X_j|X_n) = \frac{1}{K}$  with  $j = n_k + 1$  for  $1 \leq k \leq K$ , 0 otherwise.

Hyperparameters:  $K$ , distance  $d$  to compute the analogues.

<sup>9</sup>Here I follow D. Luente, J. Rolland, C. Herbert, and F. Bouchet (submitted). *J. Stat. Mech.* but the idea is much older: see E. N. Lorenz (1969). *J. Atmos. Sci.*; P. Yiou (2014). *Geosci. Model Dev.*; P. Platzer et al. (2021). *J. Atmos. Sci.*; see also D. Crommelin and E. Vanden-Eijnden (2006). *J. Comput. Phys.*

# Committer function for a Markov Chain<sup>10</sup>

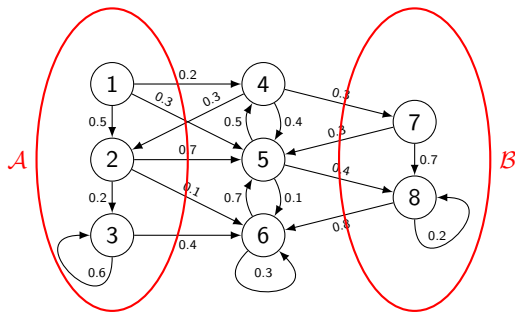
Start from transition matrix  $G$ .



<sup>10</sup>J.-H. Prinz, M. Held, J. C. Smith, and F. Noé (2011). *Multiscale Model. Simul.*

# Committor function for a Markov Chain<sup>10</sup>

Start from transition matrix  $G$ .

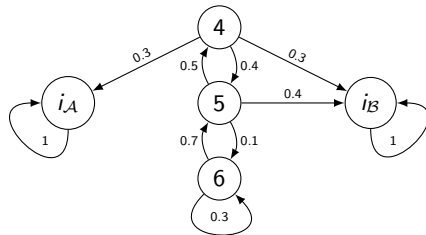


- Group all states in set  $\mathcal{A}$  and set  $\mathcal{B}$ .

<sup>10</sup>J.-H. Prinz, M. Held, J. C. Smith, and F. Noé (2011). *Multiscale Model. Simul.*

# Committer function for a Markov Chain<sup>10</sup>

Start from transition matrix  $G$ .

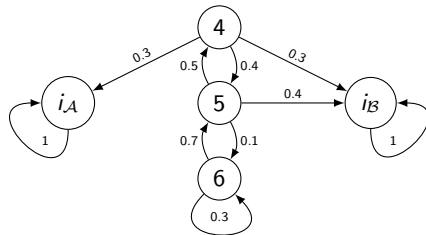


- ▶ Group all states in set  $\mathcal{A}$  and set  $\mathcal{B}$ .
- ▶ Make  $\mathcal{A}$  and  $\mathcal{B}$  absorbing.

<sup>10</sup>J.-H. Prinz, M. Held, J. C. Smith, and F. Noé (2011). *Multiscale Model. Simul.*

# Committor function for a Markov Chain<sup>10</sup>

Start from transition matrix  $G$ .



- ▶ Group all states in set  $\mathcal{A}$  and set  $\mathcal{B}$ .
- ▶ Make  $\mathcal{A}$  and  $\mathcal{B}$  absorbing.
- ▶ For the new Markov chain  $\tilde{G}$ , the committor satisfies the eigenvalue problem:

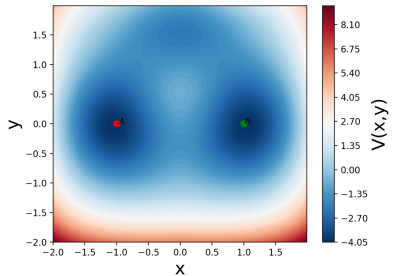
$$\tilde{G}q = q, \text{ with } q_{i_A} = 0 \text{ and } q_{i_B} = 1.$$

<sup>10</sup>J.-H. Prinz, M. Held, J. C. Smith, and F. Noé (2011). *Multiscale Model. Simul.*

# Example 1: Three-well potential<sup>11</sup>

We consider a 2D gradient system:

$$d\mathbf{x}_t = -\nabla V(\mathbf{x})dt + \sqrt{2D}d\mathbf{W}_t.$$



Two global minima  $\mathbf{x}_1, \mathbf{x}_2$ .

One local minimum  $\mathbf{x}_m$ .

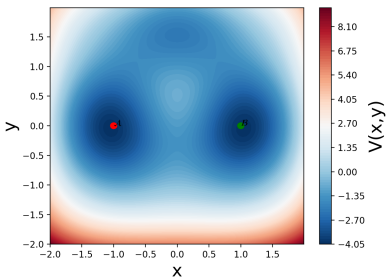
Three saddle points.

<sup>11</sup>D. Luente, J. Rolland, C. Herbert, and F. Bouchet (submitted). *J. Stat. Mech.*

# Example 1: Three-well potential<sup>11</sup>

We consider a 2D gradient system:

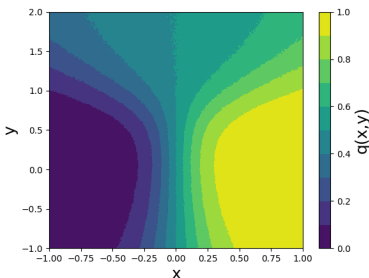
$$d\mathbf{x}_t = -\nabla V(\mathbf{x})dt + \sqrt{2D}d\mathbf{W}_t.$$



Two global minima  $\mathbf{x}_1, \mathbf{x}_2$ .  
One local minimum  $\mathbf{x}_m$ .  
Three saddle points.

Direct computation of the committor:

$$\begin{aligned}\mathcal{A} &= \{\mathbf{x} : d_E(\mathbf{x}, \mathbf{x}_1) < 0.05\}, \\ \mathcal{B} &= \{\mathbf{x} : d_E(\mathbf{x}, \mathbf{x}_2) < 0.05\}.\end{aligned}$$

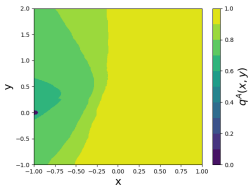


$D = 0.5$ ,  $250^2$  grid, 10 000 trajectories per grid point.

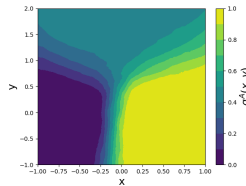
<sup>11</sup>D. Luente, J. Rolland, C. Herbert, and F. Bouchet (submitted). *J. Stat. Mech.*

# Committor function for the three-well potential from data<sup>12</sup>

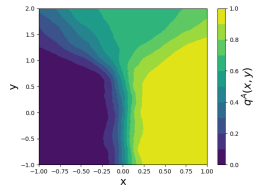
1 reactive trajectory



2 reactive trajectories



20 reactive trajectories

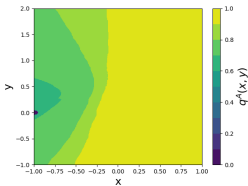


- The committor estimated with the analogue method seems to converge to the true committor as available data increase.

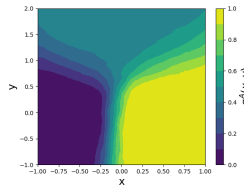
<sup>12</sup>D. Luente, J. Rolland, C. Herbert, and F. Bouchet (submitted). *J. Stat. Mech.*

# Committor function for the three-well potential from data<sup>12</sup>

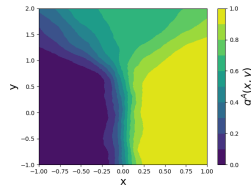
1 reactive trajectory



2 reactive trajectories



20 reactive trajectories

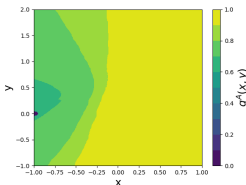


- ▶ The committor estimated with the analogue method seems to converge to the true committor as available data increase.
- ▶ The approximation is already reasonably good with a few observed reactive trajectories

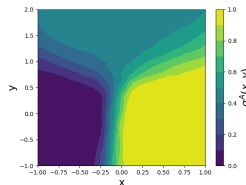
<sup>12</sup>D. Luente, J. Rolland, C. Herbert, and F. Bouchet (submitted). *J. Stat. Mech.*

# Committor function for the three-well potential from data<sup>12</sup>

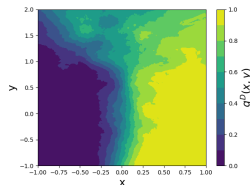
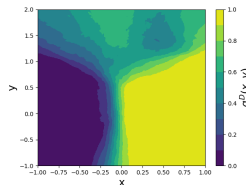
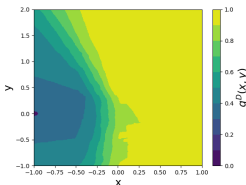
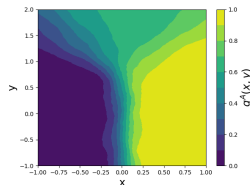
1 reactive trajectory



2 reactive trajectories



20 reactive trajectories



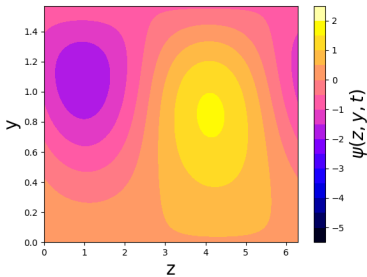
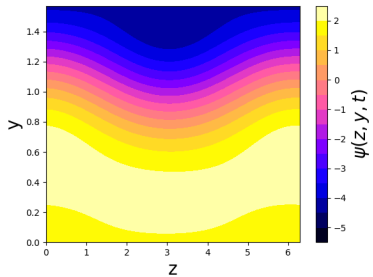
- ▶ The committor estimated with the analogue method seems to converge to the true committor as available data increase.
- ▶ The approximation is already reasonably good with a few observed reactive trajectories
- ▶ The analogue method outperforms direct estimate with the same amount of data.

<sup>12</sup>D. Luente, J. Rolland, C. Herbert, and F. Bouchet (submitted). *J. Stat. Mech.*

## Example 2: Charney-De Vore model

6-degree of freedom model for transitions between zonal and blocked atmospheric flow<sup>13</sup>.

In some parameter regime the model admits two equilibrium states<sup>14</sup>.



<sup>13</sup>J. Charney and J DeVore (1979). *J. Atmos. Sci.*

<sup>14</sup>D. T. Crommelin, J. D. Opsteegh, and F Verhulst (2004). *J. Atmos. Sci.*; T. Grafke and E. Vanden-Eijnden (2019). *Chaos*.

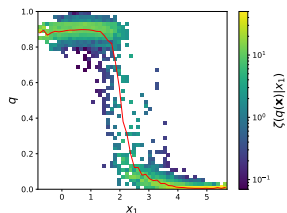
# Committor function for the Charney-De Vore model from data<sup>15</sup>

Conditional distribution of the committor:

$$\zeta(q|x_1) = \frac{\int d\mathbf{y} \rho_s(\mathbf{y}) \delta(q(\mathbf{y}) - q) \delta(y_1 - x_1)}{\int d\mathbf{y} \rho_s(\mathbf{y}) \delta(y_1 - x_1)},$$

and conditional average (red lines)  $\mathbb{E}[q|x_1] = \int q \zeta(q|x_1) dq$ .

## Direct Estimate



<sup>15</sup>D. Luente, J. Rolland, C. Herbert, and F. Bouchet (submitted). *J. Stat. Mech.*

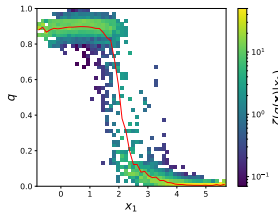
Committor function for the Charney-De Vore model from data<sup>15</sup>

Conditional distribution of the committer:

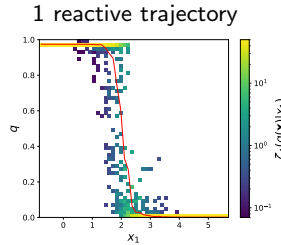
$$\zeta(q|x_1) = \frac{\int d\mathbf{y} \rho_s(\mathbf{y}) \delta(q(\mathbf{y}) - q) \delta(y_1 - x_1)}{\int d\mathbf{y} \rho_s(\mathbf{y}) \delta(y_1 - x_1)},$$

and conditional average (red lines)  $\mathbb{E}[q|x_1] = \int q\zeta(q|x_1)dq$ .

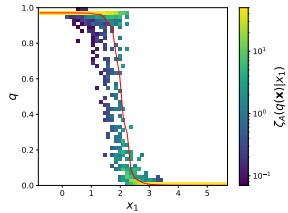
## Direct Estimate



## Analogue Method



## 15 reactive trajectories



<sup>15</sup>D. Luente, J. Rolland, C. Herbert, and F. Bouchet (submitted). *J. Stat. Mech.*

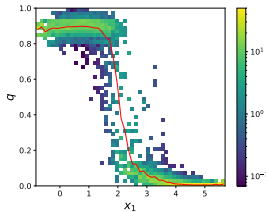
# Committor function for the Charney-De Vore model from data<sup>15</sup>

Conditional distribution of the committor:

$$\zeta(q|x_1) = \frac{\int d\mathbf{y} \rho_s(\mathbf{y}) \delta(q(\mathbf{y}) - q) \delta(y_1 - x_1)}{\int d\mathbf{y} \rho_s(\mathbf{y}) \delta(y_1 - x_1)},$$

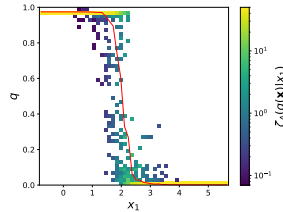
and conditional average (red lines)  $\mathbb{E}[q|x_1] = \int q \zeta(q|x_1) dq$ .

Direct Estimate

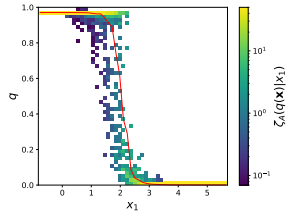


Analogue Method

1 reactive trajectory



15 reactive trajectories



*Qualitative structure of committor function captured by the analogue method, even for small dataset.*

<sup>15</sup>D. Lucente, J. Rolland, C. Herbert, and F. Bouchet (submitted). *J. Stat. Mech.*

# Some other data-based methods to estimate committer functions

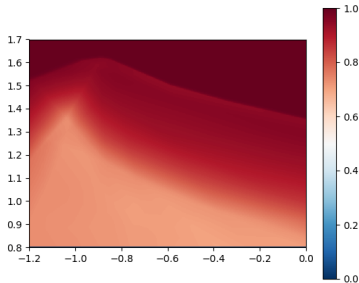
## ► Committer function regression with a neural network

Multilayer Perceptron with cost Function:

$$C = -\frac{1}{N} \sum_{n=1}^N [y_n \ln \hat{q}_{NN}(\mathbf{x}_n) + (1 - y_n) \ln(1 - \hat{q}_{NN}(\mathbf{x}_n))], \text{ with}$$
$$y_n = \Theta(\tau_A(\mathbf{x}_n) - \tau_B(\mathbf{x}_n)).$$

Lucente, Duffner, Herbert, Rolland, and Bouchet 2019

Application to the Jin-Timmerman model,  $\sigma = 10^{-3}$ :



# Some other data-based methods to estimate committor functions

- ▶ Committor function regression with a neural network

Multilayer Perceptron with cost Function:

$$C = -\frac{1}{N} \sum_{n=1}^N [y_n \ln \hat{q}_{NN}(\mathbf{x}_n) + (1 - y_n) \ln(1 - \hat{q}_{NN}(\mathbf{x}_n))], \text{ with}$$
$$y_n = \Theta(\tau_A(\mathbf{x}_n) - \tau_B(\mathbf{x}_n)).$$

Lucente, Duffner, Herbert, Rolland, and Bouchet 2019

- ▶ Application to heat wave prediction

V. Jacques-Dumas, F. Ragone, P. Borgnat, P. Abry, and F. Bouchet (2022). *Front. Clim.*

G. Miloshevich et al. upcoming

# Some other data-based methods to estimate committor functions

- ▶ Committor function regression with a neural network

Multilayer Perceptron with cost Function:

$$C = -\frac{1}{N} \sum_{n=1}^N [y_n \ln \hat{q}_{NN}(\mathbf{x}_n) + (1 - y_n) \ln(1 - \hat{q}_{NN}(\mathbf{x}_n))], \text{ with}$$
$$y_n = \Theta(\tau_A(\mathbf{x}_n) - \tau_B(\mathbf{x}_n)).$$

Lucente, Duffner, Herbert, Rolland, and Bouchet 2019

- ▶ Application to heat wave prediction

V. Jacques-Dumas, F. Ragone, P. Borgnat, P. Abry, and F. Bouchet (2022). *Front. Clim.*

G. Miloshevich et al. upcoming

- ▶ Data-based approximation of the eigenmodes of the generator/Koopman operator.

E. H. Thiede, D. Giannakis, A. R. Dinner, and J. Weare (2019). *J. Chem. Phys.*

J. Finkel, R. J. Webber, E. P. Gerber, D. S. Abbot, and J. Weare (2021). *Mon. Wea. Rev.*

# Some other data-based methods to estimate committor functions

- ▶ Committor function regression with a neural network

Multilayer Perceptron with cost Function:

$$C = -\frac{1}{N} \sum_{n=1}^N [y_n \ln \hat{q}_{NN}(\mathbf{x}_n) + (1 - y_n) \ln(1 - \hat{q}_{NN}(\mathbf{x}_n))], \text{ with}$$
$$y_n = \Theta(\tau_A(\mathbf{x}_n) - \tau_B(\mathbf{x}_n)).$$

Lucente, Duffner, Herbert, Rolland, and Bouchet 2019

- ▶ Application to heat wave prediction

V. Jacques-Dumas, F. Ragone, P. Borgnat, P. Abry, and F. Bouchet (2022). *Front. Clim.*

G. Miloshevich et al. upcoming

- ▶ Data-based approximation of the eigenmodes of the generator/Koopman operator.

E. H. Thiede, D. Giannakis, A. R. Dinner, and J. Weare (2019). *J. Chem. Phys.*

J. Finkel, R. J. Webber, E. P. Gerber, D. S. Abbot, and J. Weare (2021). *Mon. Wea. Rev.*

- ▶ Machine learning solution of the Kolmogorov equation for the committor.

Y. Khoo, J. Lu, and L. Ying (2019). *Res. Math. Sci.*

# Some other data-based methods to estimate committor functions

- ▶ Committor function regression with a neural network

Multilayer Perceptron with cost Function:

$$C = -\frac{1}{N} \sum_{n=1}^N [y_n \ln \hat{q}_{NN}(\mathbf{x}_n) + (1 - y_n) \ln(1 - \hat{q}_{NN}(\mathbf{x}_n))], \text{ with}$$
$$y_n = \Theta(\tau_A(\mathbf{x}_n) - \tau_B(\mathbf{x}_n)).$$

Lucente, Duffner, Herbert, Rolland, and Bouchet 2019

- ▶ Application to heat wave prediction

V. Jacques-Dumas, F. Ragone, P. Borgnat, P. Abry, and F. Bouchet (2022). *Front. Clim.*

G. Miloshevich et al. upcoming

- ▶ Data-based approximation of the eigenmodes of the generator/Koopman operator.

E. H. Thiede, D. Giannakis, A. R. Dinner, and J. Weare (2019). *J. Chem. Phys.*

J. Finkel, R. J. Webber, E. P. Gerber, D. S. Abbot, and J. Weare (2021). *Mon. Wea. Rev.*

- ▶ Machine learning solution of the Kolmogorov equation for the committor.

Y. Khoo, J. Lu, and L. Ying (2019). *Res. Math. Sci.*

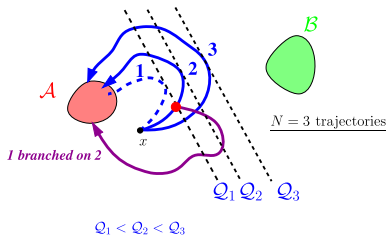
- ▶ ...

# Outline

- 1 Introduction: Committor functions for Prediction Problems and Climate Transitions
- 2 Climate prediction at the predictability margin
- 3 Data-based methods for committer function computation
- 4 Rare events and committer functions
- 5 Conclusion

# The AMS algorithm<sup>16</sup>

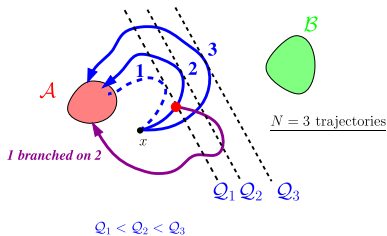
Ensemble  $\{x_n^{(0)}(t)\}$  of  $N$  independent trajectories, weight  $w_0 = 1$ .



<sup>16</sup>F. Cérou and A. Guyader (2007). *Stoch. Anal. Appl.*

# The AMS algorithm<sup>16</sup>

Ensemble  $\{x_n^{(0)}(t)\}$  of  $N$  independent trajectories, weight  $w_0 = 1$ .



*Selection-mutation* steps, with *score function*  $\phi$ : at iteration  $j \geq 1$ ,

- ▶ *Selection.* trajectory  $n_j^*$  with the lowest score:

$$Q_{n_j^*}^{(j)} = \min_{1 \leq n \leq N} Q_n^{(j)}, \text{ with } Q_n^{(j)} = \sup_t \phi(t, x_n^{(j-1)}(t)).$$

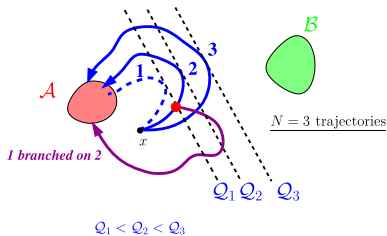
- ▶ *Mutation.* Resimulate the trajectory starting from the threshold  $Q_{n_j^*}^{(j)}$ .

Associate weight  $w_j = (1 - 1/N)w_{j-1}$  to the trajectories in the ensemble.

<sup>16</sup>F. Cérou and A. Guyader (2007). *Stoch. Anal. Appl.*

# The AMS algorithm<sup>16</sup>

Ensemble  $\{x_n^{(0)}(t)\}$  of  $N$  independent trajectories, weight  $w_0 = 1$ .



*Selection-mutation* steps, with *score function*  $\phi$ : at iteration  $j \geq 1$ ,

- ▶ *Selection.* trajectory  $n_j^*$  with the lowest score:

$$Q_{n_j^*}^{(j)} = \min_{1 \leq n \leq N} Q_n^{(j)}, \text{ with } Q_n^{(j)} = \sup_t \phi(t, x_n^{(j-1)}(t)).$$

- ▶ *Mutation.* Resimulate the trajectory starting from the threshold  $Q_{n_j^*}^{(j)}$ .

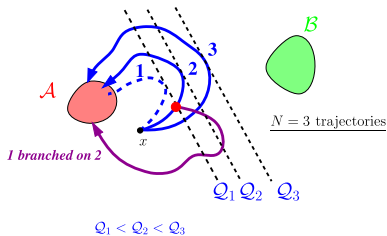
Associate weight  $w_j = (1 - 1/N)w_{j-1}$  to the trajectories in the ensemble.

Iterate until all trajectories reach set  $\mathcal{B}$ .

<sup>16</sup>F. Cérou and A. Guyader (2007). *Stoch. Anal. Appl.*

# The AMS algorithm<sup>16</sup>

Ensemble  $\{x_n^{(0)}(t)\}$  of  $N$  independent trajectories, weight  $w_0 = 1$ .



*Selection-mutation* steps, with *score function*  $\phi$ : at iteration  $j \geq 1$ ,

- ▶ *Selection.* trajectory  $n_j^*$  with the lowest score:

$$Q_{n_j^*}^{(j)} = \min_{1 \leq n \leq N} Q_n^{(j)}, \text{ with } Q_n^{(j)} = \sup_t \phi(t, x_n^{(j-1)}(t)).$$

- ▶ *Mutation.* Resimulate the trajectory starting from the threshold  $Q_{n_j^*}^{(j)}$ .

Associate weight  $w_j = (1 - 1/N)w_{j-1}$  to the trajectories in the ensemble.

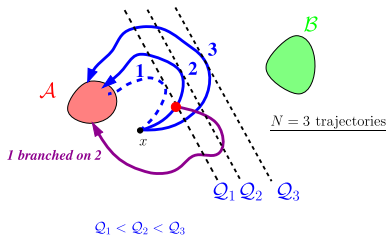
Iterate until all trajectories reach set  $\mathcal{B}$ .

Transition probability estimator  $\hat{\alpha} = w_J = \prod_{j=1}^J \left(1 - \frac{1}{N}\right)$ .

<sup>16</sup>F. Cérou and A. Guyader (2007). *Stoch. Anal. Appl.*

# The AMS algorithm<sup>16</sup>

Ensemble  $\{x_n^{(0)}(t)\}$  of  $N$  independent trajectories, weight  $w_0 = 1$ .



**Selection-mutation** steps, with **score function**  $\phi$ : at iteration  $j \geq 1$ ,

- ▶ **Selection.** trajectory  $n_j^*$  with the lowest score:

$$\mathcal{Q}_{n_j^*}^{(j)} = \min_{1 \leq n \leq N} \mathcal{Q}_n^{(j)}, \text{ with } \mathcal{Q}_n^{(j)} = \sup_t \phi(t, x_n^{(j-1)}(t)).$$

- ▶ **Mutation.** Resimulate the trajectory starting from the threshold  $\mathcal{Q}_{n_j^*}^{(j)}$ .

Associate weight  $w_j = (1 - 1/N)w_{j-1}$  to the trajectories in the ensemble.

Iterate until all trajectories reach set  $\mathcal{B}$ .

Transition probability estimator  $\hat{\alpha} = w_j = \prod_{j=1}^J \left(1 - \frac{1}{N}\right)$ .

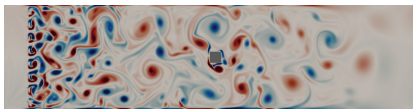
**The choice of a good score function is crucial**

<sup>16</sup>F. Cérou and A. Guyader (2007). *Stoch. Anal. Appl.*

# The extinction problem

## Grid turbulence

2D channel flow with square obstacle in the middle of the domain, simulated with a Lattice Boltzmann method<sup>17</sup>.

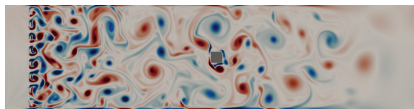


<sup>17</sup>T. Lestang, F. Bouchet, and E. Lévéque (2020). *J. Fluid Mech.*

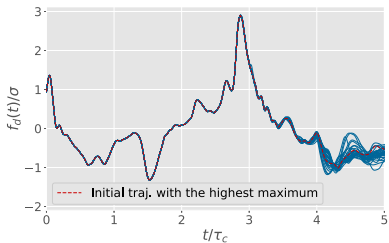
# The extinction problem

## Grid turbulence

2D channel flow with square obstacle in the middle of the domain, simulated with a Lattice Boltzmann method<sup>17</sup>.



## Drag force exerted on the square

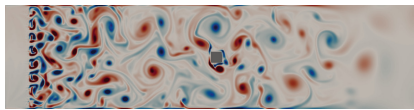


<sup>17</sup>T. Lestang, F. Bouchet, and E. Lévéque (2020). *J. Fluid Mech.*

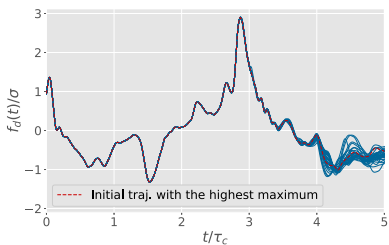
# The extinction problem

## Grid turbulence

2D channel flow with square obstacle in the middle of the domain, simulated with a Lattice Boltzmann method<sup>17</sup>.



## Drag force exerted on the square



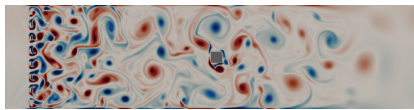
Resampled trajectories never exceed the maximum in the initial ensemble, leading to *extinction* (all trajectories should be killed at once).  
This is because the instantaneous drag force is not a good predictor of the occurrence of extreme drag in the future.

<sup>17</sup>T. Lestang, F. Bouchet, and E. Lévéque (2020). *J. Fluid Mech.*

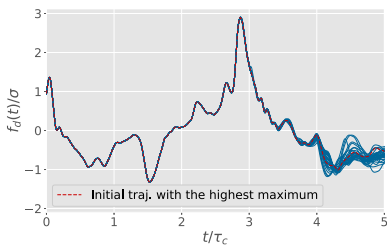
# The extinction problem

## Grid turbulence

2D channel flow with square obstacle in the middle of the domain, simulated with a Lattice Boltzmann method<sup>17</sup>.



## Drag force exerted on the square



Resampled trajectories never exceed the maximum in the initial ensemble, leading to *extinction* (all trajectories should be killed at once). This is because the instantaneous drag force is not a good predictor of the occurrence of extreme drag in the future.

*Can we use available data to construct good score functions?*

<sup>17</sup>T. Lestang, F. Bouchet, and E. Lévéque (2020). *J. Fluid Mech.*

# The apparent bias problem

## Properties of the transition probability estimator<sup>18</sup>

- ▶ Unbiased estimator:  $\mathbb{E}[\hat{\alpha}] = \alpha$  for all  $N$  and  $\phi$
- ▶ The score function which minimizes the variance  $\sigma^2 = \mathbb{E}[(\hat{\alpha} - \alpha)^2]$  is the committor function. Then  $\sigma \sim_{N \rightarrow \infty} \frac{\alpha \sqrt{|\ln \alpha|}}{\sqrt{N}}$ .

<sup>18</sup>e.g. C.-E. Bréhier, M. Gazeau, L. Goudenège, T. Lelièvre, and M. Rousset (2016). *Ann. Appl. Probab.*

# The apparent bias problem

## Properties of the transition probability estimator<sup>18</sup>

- ▶ Unbiased estimator:  $\mathbb{E}[\hat{\alpha}] = \alpha$  for all  $N$  and  $\phi$
- ▶ The score function which minimizes the variance  $\sigma^2 = \mathbb{E}[(\hat{\alpha} - \alpha)^2]$  is the committor function. Then  $\sigma \sim_{N \rightarrow \infty} \frac{\alpha \sqrt{|\ln \alpha|}}{\sqrt{N}}$ .

## Apparent bias phenomenon<sup>19</sup>

For some score functions, the empirical average systematically underestimates the transition probability  $\alpha$ :

$$\frac{1}{M} \sum_{m=1}^M \hat{\alpha}^{(M)} < \alpha.$$

<sup>18</sup>e.g. C.-E. Bréhier, M. Gazeau, L. Goudenège, T. Lelièvre, and M. Rousset (2016). *Ann. Appl. Probab.*

<sup>19</sup>J. Rolland and E. Simonnet (2015). *J. Comput. Phys.*

# The apparent bias problem

## Properties of the transition probability estimator<sup>18</sup>

- ▶ Unbiased estimator:  $\mathbb{E}[\hat{\alpha}] = \alpha$  for all  $N$  and  $\phi$
- ▶ The score function which minimizes the variance  $\sigma^2 = \mathbb{E}[(\hat{\alpha} - \alpha)^2]$  is the committor function. Then  $\sigma \sim_{N \rightarrow \infty} \frac{\alpha \sqrt{|\ln \alpha|}}{\sqrt{N}}$ .

## Apparent bias phenomenon<sup>19</sup>

For some score functions, the empirical average systematically underestimates the transition probability  $\alpha$ :

$$\frac{1}{M} \sum_{m=1}^M \hat{\alpha}^{(M)} < \alpha.$$

*Can data-based score functions make rare event algorithms more precise?*

<sup>18</sup>e.g. C.-E. Bréhier, M. Gazeau, L. Goudenège, T. Lelièvre, and M. Rousset (2016). *Ann. Appl. Probab.*

<sup>19</sup>J. Rolland and E. Simonnet (2015). *J. Comput. Phys.*

# The apparent bias problem

## Properties of the transition probability estimator<sup>18</sup>

- ▶ Unbiased estimator:  $\mathbb{E}[\hat{\alpha}] = \alpha$  for all  $N$  and  $\phi$
- ▶ The score function which minimizes the variance  $\sigma^2 = \mathbb{E}[(\hat{\alpha} - \alpha)^2]$  is the committor function. Then  $\sigma \sim_{N \rightarrow \infty} \frac{\alpha \sqrt{|\ln \alpha|}}{\sqrt{N}}$ .

## Apparent bias phenomenon<sup>19</sup>

For some score functions, the empirical average systematically underestimates the transition probability  $\alpha$ :

$$\frac{1}{M} \sum_{m=1}^M \hat{\alpha}^{(M)} < \alpha.$$

*Can data-based score functions make rare event algorithms more precise?*

## Other observables

Because the AMS samples trajectories, we can estimate any observable. Here we will consider the average duration of reactive trajectories  $\tau$ .

<sup>18</sup>e.g. C.-E. Bréhier, M. Gazeau, L. Goudenègue, T. Lelièvre, and M. Rousset (2016). *Ann. Appl. Probab.*

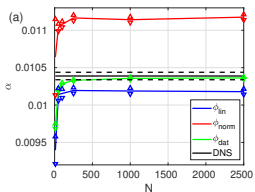
<sup>19</sup>J. Rolland and E. Simonnet (2015). *J. Comput. Phys.*

## Performance of the learned score function for the three-well model<sup>20</sup>

## Convergence of AMS estimates with the number of clones

We compare the analogue score function  $\phi_{dat}$  with prescribed score functions

$$\phi_{lin}(x, y) = \frac{x+1}{2}, \quad \phi_{norm}(x, y) = \frac{1}{2} \sqrt{(x+1)^2 + \frac{y^2}{2}}.$$



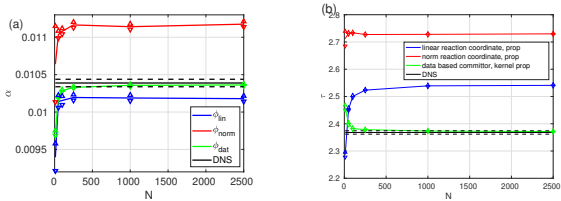
<sup>20</sup>D. Lucente, J. Rolland, C. Herbert, and F. Bouchet (submitted). *J. Stat. Mech.*

Performance of the learned score function for the three-well model<sup>20</sup>

## Convergence of AMS estimates with the number of clones

We compare the analogue score function  $\phi_{dat}$  with prescribed score functions

$$\phi_{lin}(x, y) = \frac{x+1}{2}, \quad \phi_{norm}(x, y) = \frac{1}{2} \sqrt{(x+1)^2 + \frac{y^2}{2}}.$$



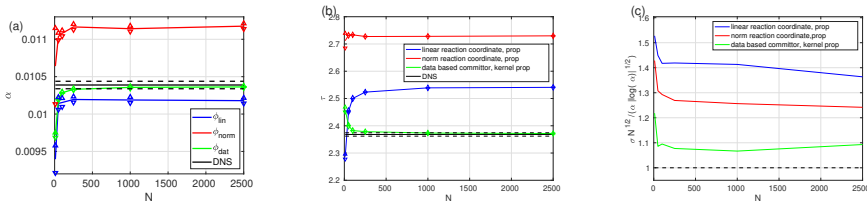
<sup>20</sup>D. Luente, J. Rolland, C. Herbert, and F. Bouchet (submitted). *J. Stat. Mech.*

## Performance of the learned score function for the three-well model<sup>20</sup>

## Convergence of AMS estimates with the number of clones

We compare the analogue score function  $\phi_{dat}$  with prescribed score functions

$$\phi_{lin}(x, y) = \frac{x+1}{2}, \quad \phi_{norm}(x, y) = \frac{1}{2} \sqrt{(x+1)^2 + \frac{y^2}{2}}.$$



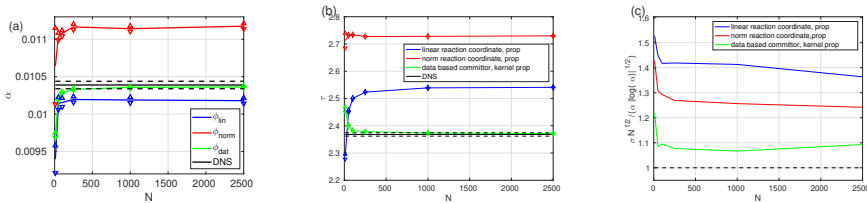
<sup>20</sup>D. Luente, J. Rolland, C. Herbert, and F. Bouchet (submitted). *J. Stat. Mech.*

## Performance of the learned score function for the three-well model<sup>20</sup>

## Convergence of AMS estimates with the number of clones

We compare the analogue score function  $\phi_{dat}$  with prescribed score functions

$$\phi_{lin}(x, y) = \frac{x+1}{2}, \quad \phi_{norm}(x, y) = \frac{1}{2} \sqrt{(x+1)^2 + \frac{y^2}{2}}.$$



*The analogue score function does not suffer from the “apparent bias” phenomenon, unlike user-defined score functions.*

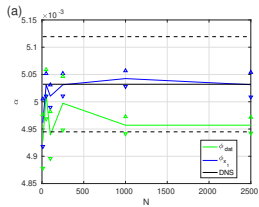
<sup>20</sup>D. Luente, J. Rolland, C. Herbert, and F. Bouchet (submitted). *J. Stat. Mech.*

Performance of the learned score function for the Charney-De Vore model<sup>21</sup>

## Convergence of AMS estimates with the number of clones

We compare the analogue score function  $\phi_{dat}$  with a prescribed score function

$$\phi_{x_1}(\mathbf{x}) = \frac{x_1 - x_{1,Z}}{x_{1,B} - x_{1,Z}}.$$



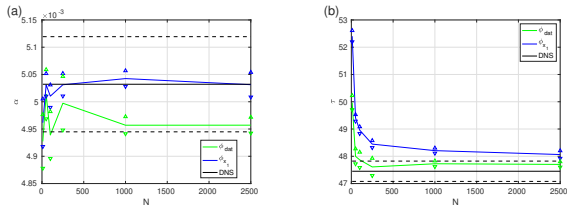
<sup>21</sup>D. Lucente, J. Rolland, C. Herbert, and E. Bouchet (submitted). *J. Stat. Mech.*

Performance of the learned score function for the Charney-De Vore model<sup>21</sup>

## Convergence of AMS estimates with the number of clones

We compare the analogue score function  $\phi_{dat}$  with a prescribed score function

$$\phi_{x_1}(\mathbf{x}) = \frac{x_1 - x_{1,Z}}{x_{1,B} - x_{1,Z}}.$$



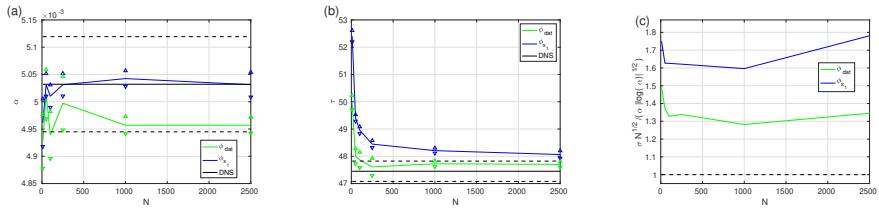
<sup>21</sup>D. Luente, J. Rolland, C. Herbert, and E. Bouchet (submitted). *J. Stat. Mech.*

Performance of the learned score function for the Charney-De Vore model<sup>21</sup>

## Convergence of AMS estimates with the number of clones

We compare the analogue score function  $\phi_{dat}$  with a prescribed score function

$$\phi_{x_1}(\mathbf{x}) = \frac{x_1 - x_{1,Z}}{x_{1,B} - x_{1,Z}}.$$

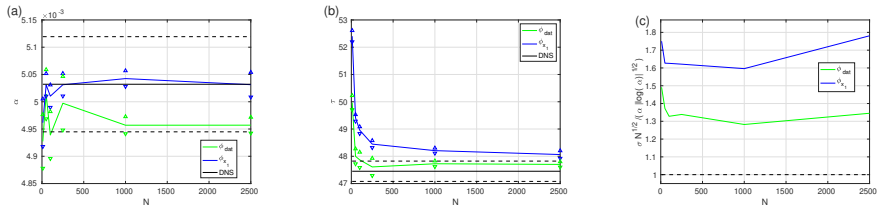


Performance of the learned score function for the Charney-De Vore model<sup>21</sup>

## Convergence of AMS estimates with the number of clones

We compare the analogue score function  $\phi_{dat}$  with a prescribed score function

$$\phi_{x_1}(\mathbf{x}) = \frac{x_1 - x_{1,Z}}{x_{1,B} - x_{1,Z}}.$$

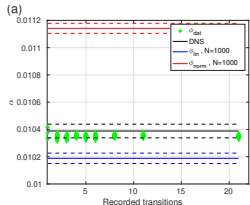


*Similar conclusions hold for the Charney-De Vore model.*

<sup>21</sup>D. Luente, J. Rolland, C. Herbert, and F. Bouchet (submitted). *J. Stat. Mech.*

Role of the amount of data used to learn the score function<sup>22</sup>

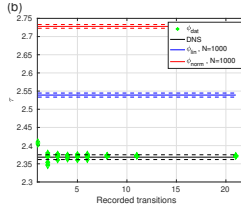
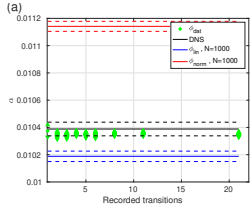
## Three-well model



<sup>22</sup>D. Luente, J. Rolland, C. Herbert, and F. Bouchet (submitted). *J. Stat. Mech.*

# Role of the amount of data used to learn the score function<sup>22</sup>

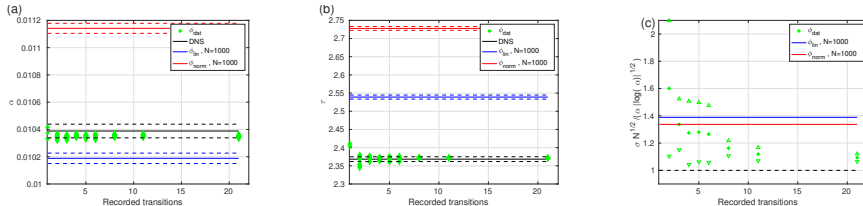
## Three-well model



<sup>22</sup>D. Luente, J. Rolland, C. Herbert, and F. Bouchet (submitted). *J. Stat. Mech.*

Role of the amount of data used to learn the score function<sup>22</sup>

## Three-well model

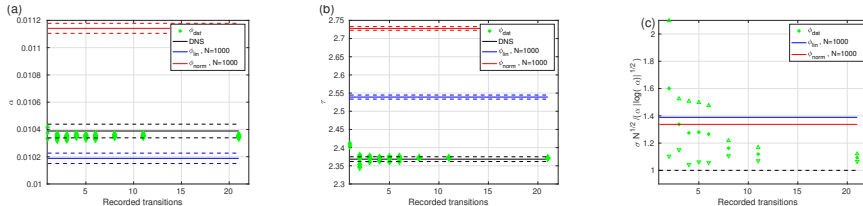


*Data-based score function already yields precise results for small dataset.*

<sup>22</sup>R. Luente, J. Rolland, C. Herbert, and F. Bouchet (submitted), *J. Stat. Mech.*

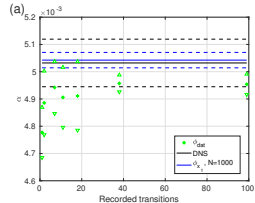
Role of the amount of data used to learn the score function<sup>22</sup>

## Three-well model



*Data-based score function already yields precise results for small dataset.*

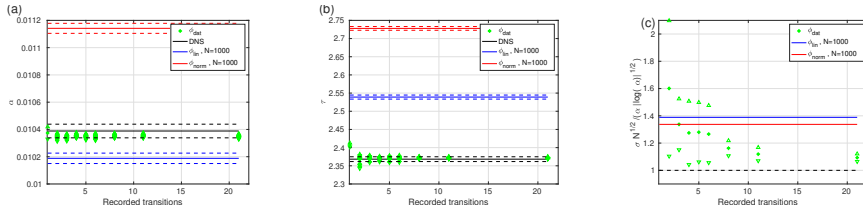
## Charney-De Vore model



<sup>22</sup>R. Luente, J. Rolland, C. Herbert, and F. Bouchet (submitted), *J. Stat. Mech.*

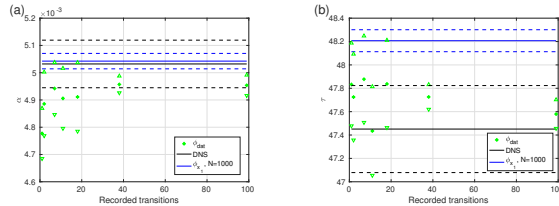
Role of the amount of data used to learn the score function<sup>22</sup>

## Three-well model



*Data-based score function already yields precise results for small dataset.*

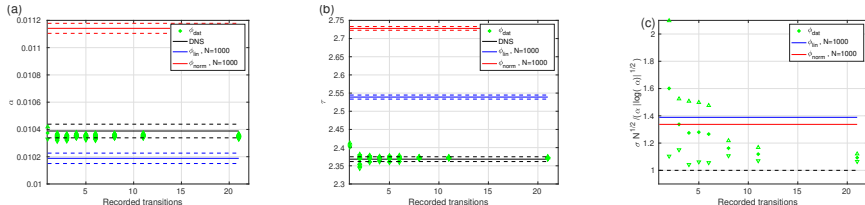
## Charney-De Vore model



<sup>22</sup>D. Lucente, J. Rolland, C. Herbert, and E. Bouchet (submitted), *J. Stat. Mech.*

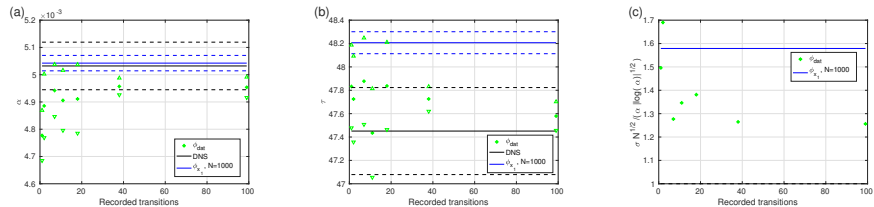
Role of the amount of data used to learn the score function<sup>22</sup>

## Three-well model



*Data-based score function already yields precise results for small dataset.*

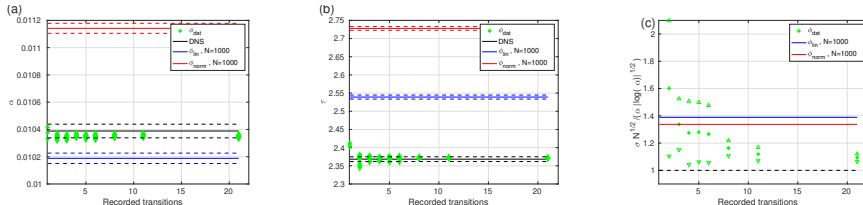
## Charney-De Vore model



<sup>22</sup>D. Lucente, J. Rolland, C. Herbert, and E. Bouchet (submitted). *J. Stat. Mech.*

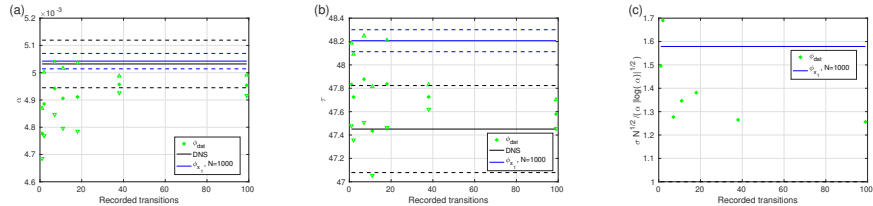
Role of the amount of data used to learn the score function<sup>22</sup>

## Three-well model



*Data-based score function already yields precise results for small dataset.*

## Charney-De Vore model



Here increasing the amount of data used for the score function decreases the variability of AMS estimates.

<sup>22</sup>D. Luente, J. Rolland, C. Herbert, and F. Bouchet (submitted), *J. Stat. Mech.*

## Summary & Conclusions

- ▶ For strong EL Niño events in the Jin-Timmermann model, we observe *regions in phase space where probabilistic prediction is possible* (“smooth” committor) and other *regions where the probability of occurrence of the event depends sensitively on the initial condition* (“rough committor”).
- ▶ We need efficient ways to estimate committor functions in high-dimensional systems from data, sampled either directly or through rare event algorithms.  
We presented one such method based on constructing an effective dynamics using the *analogue method*.  
Other methods are possible, for instance based on *machine learning*.
- ▶ *Using a data-based score function makes the AMS easier to use and more precise.*  
The score function may be improved iteratively by coupling rare event algorithm with committor learning methods.



- Baars, S., D Castellana, F. W. Wubs, and H. A. Dijkstra (2021). *J. Comput. Phys.* 424, p. 109876.
- Bouchet, F., J. Rolland, and E. Simonnet (2019). *Phys. Rev. Lett.* 122, p. 074502.
- Bréhier, C.-E., M. Gazeau, L. Goudenègue, T. Lelièvre, and M. Rousset (2016). *Ann. Appl. Probab.* 26.6, pp. 3559–3601. ISSN: 1050-5164.
- Cassou, C. (2008). *Nature* 455.7212, pp. 523–527.
- Cérou, F. and A. Guyader (2007). *Stoch. Anal. Appl.* 25, pp. 417–443.
- Charney, J. and J DeVore (1979). *J. Atmos. Sci.* 36, p. 1205.
- Crommelin, D. T., J. D. Opsteegh, and F Verhulst (2004). *J. Atmos. Sci.* 61.12, pp. 1406–1419.
- Crommelin, D. and E. Vanden-Eijnden (2006). *J. Comput. Phys.* 217.2, pp. 782–805.
- Finkel, J., R. J. Webber, E. P. Gerber, D. S. Abbot, and J. Weare (2021). *Mon. Wea. Rev.* 149.11, pp. 3647–3669.
- Grafke, T. and E. Vanden-Eijnden (2019). *Chaos* 29.6, p. 063118.
- Guckenheimer, J., A. Timmermann, H. Dijkstra, and A. Roberts (2017). *Dyn. Stat. Clim. Sys.* 2.1, dzx004.
- Herbert, C., R. Caballero, and F. Bouchet (2020). *J. Atmos. Sci.* 77, pp. 31–49.
- Jacques-Dumas, V., F. Ragone, P. Borgnat, P. Abry, and F. Bouchet (2022). *Front. Clim.*
- Jin, F.-F. (1997a). *J. Atmos. Sci.* 54.7, pp. 811–829.
- (1997b). *J. Atmos. Sci.* 54.7, pp. 830–847.
- Khoo, Y., J. Lu, and L. Ying (2019). *Res. Math. Sci.* 6.1, pp. 1–13.
- Lestang, T., F. Bouchet, and E. Lévéque (2020). *J. Fluid Mech.* 895.
- Lestang, T., F. Ragone, C.-E. Bréhier, C. Herbert, and F. Bouchet (2018). *J. Stat. Mech.* 043213.
- Lopes, L. J. and T. Lelièvre (2019). *Journal of computational chemistry* 40.11, pp. 1198–1208.
- Lorenz, E. N. (1969). *J. Atmos. Sci.* 26.4, pp. 636–646.
- Lucente, D., S. Duffner, C. Herbert, J. Rolland, and F. Bouchet (2019). In: *Proceedings of the 9th International Workshop on Climate Informatics: CI 2019* (Paris). Ed. by J. Brajard, A. Charantonis, C. Chen, and J. Runge. NCAR. eprint: 1910.11736.
- Lucente, D., C. Herbert, and F. Bouchet (submitted). *J. Atmos. Sci.*
- Lucente, D., J. Rolland, C. Herbert, and F. Bouchet (submitted). *J. Stat. Mech.*
- Metzner, P., C. Schütte, and E. Vanden-Eijnden (2006). *J. Chem. Phys.* 125.8, p. 084110.
- Platzer, P. et al. (2021). *J. Atmos. Sci.* 78.7, pp. 2117–2133.
- Prinz, J.-H., M. Held, J. C. Smith, and F. Noé (2011). *Multiscale Model. Simul.* 9.2, pp. 545–567.
- Ragone, F., J. Wouters, and F. Bouchet (2018). *Proc. Natl. Acad. Sci. U.S.A.* 115.1, pp. 24–29.
- Roberts, A., J. Guckenheimer, E. Widiasih, A. Timmermann, and C. K. Jones (2016). *J. Atmos. Sci.* 73.4, pp. 1755–1766.
- Rolland, J. and E. Simonnet (2015). *J. Comput. Phys.* 283, pp. 541–558.
- Thiede, E. H., D. Giannakis, A. R. Dinner, and J. Weare (2019). *J. Chem. Phys.* 150.24, p. 244111.
- Timmermann, A. and F.-F. Jin (2002). *Geophys. Res. Lett.* 29.1, pp. 3–1.
- Timmermann, A., F.-F. Jin, and J. Abschagen (2003). *J. Atmos. Sci.* 60.1, pp. 152–165.
- Vanden-Eijnden, E. (2006). In: *Computer Simulations in Condensed Matter Systems: From Materials to Chemical Biology Volume 1*. Springer, pp. 453–493.
- Wang, P., D. Castellana, and H. A. Dijkstra (2021). *Nonlin. Processes Geophys.* 28.1, pp. 135–151.
- Yiou, P. (2014). *Geosci. Model Dev.* 7.2, pp. 531–543.